A Top-down Strategy Identifying Molecular Phase Stabilizers to Overcome Microstructure Instabilities in Organic Solar Cells

Chaohong Zhang,*[a,b] Thomas Heumueller,[b] Salvador Leon,[c] Wolfgang Gruber,[d] Klaus Burlafinger,[b] Xiaofeng Tang,[b] Jose D. Perea,[b] Isabell Wabra,[e] Andreas Hirsch,[e] Tobias Unruh,[d] Ning Li,*[b,f] Christoph J. Brabec *[b,g]

[a] SUSTech Academy for Advanced Interdisciplinary Studies, Southern University of Science and Technology, No. 1088, Xueyuan Rd., 518055, Shenzhen, Guangdong, China
[b] Institute of Materials for Electronics and Energy Technology (i-MEET), Friedrich-Alexander University Erlangen-Nürnberg, Martensstrasse 7, 91058 Erlangen, Germany
[c] Departmento de Ingeniería Química, Universidad Politécnica de Madrid, ETSIIM, José Gutiérrez Abascal 2, 28006 Madrid, Spain
[d] Institute for Crystallography and Structure Physics, Friedrich-Alexander University Erlangen- Nürnberg, Staudtstrasse 3, 91058 Erlangen, Germany
[e] Institute of Organic Chemistry II, Friedrich-Alexander University Erlangen-Nürnberg, Nikolaus-Fiebiger-Straße 10, 91058 Erlangen, Germany
[f] National Engineering Research Center for Advanced Polymer Processing Technology, Zhengzhou University, 450002 Zhengzhou, China
[g] Bavarian Center for Applied Energy Research (ZAE Bayern), Immerwahrstr. 2, 91058 Erlangen, Germany

* E-mail: zhangch3@sustc.edu.cn; ning.li@fau.de; christoph.brabec@fau.de;

Key words: stability of organic solar cells, bulk-heterojunction, donor-acceptor demixing, solid additive, molecular phase stabilizer, interaction parameter

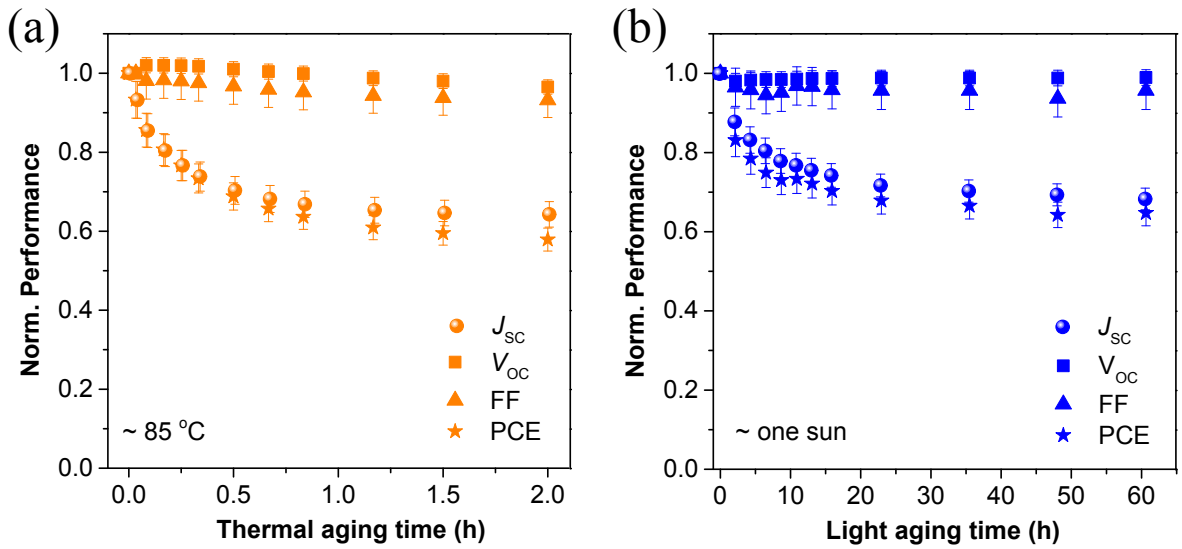

Figure S1. Normalized J_{SC}, V_{OC}, FF and PCE evolution of PCE11:$PC_{71}BM$ solar cells (a) at 85 °C annealing and (b) under white light illumination (~ one sun).

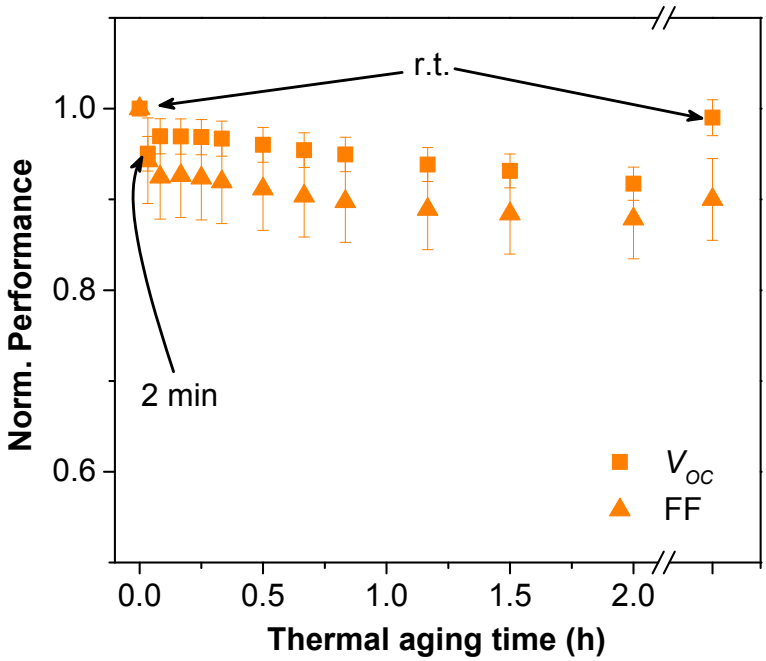

Figure S2. Normalized V_{OC} and FF evolution of PCE11:$PC_{71}BM$ solar cells under 85 °C annealing. The first point was measured at room temperature (r.t.); the second point was measured at the 2nd minute after turning on heating (temperature stabilized at 85 °C); after 2 hours' annealing, the solar cells were cooled down to room temperature (last point

in the figure). The V_{OC} and FF were temperature dependent and reversible. Thus, V_{OC} and FF evolution in Figure 1d were normalized to the point measured at the second minute.

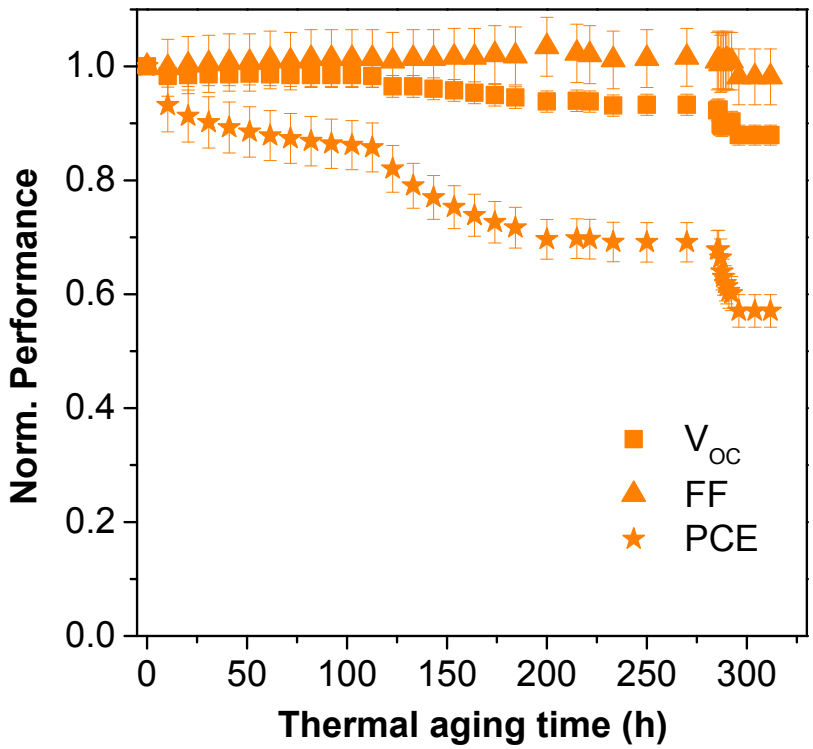

Figure S3. Normalized V_{OC}, FF and PCE evolution of PCE11:$PC_{71}BM$ solar cells aged at varying temperature in nitrogen atmosphere. The V_{OC} decreased whenever the temperature increased because of the temperature-dependent effects, which is was found to be reversible as depicted in Figure S2.

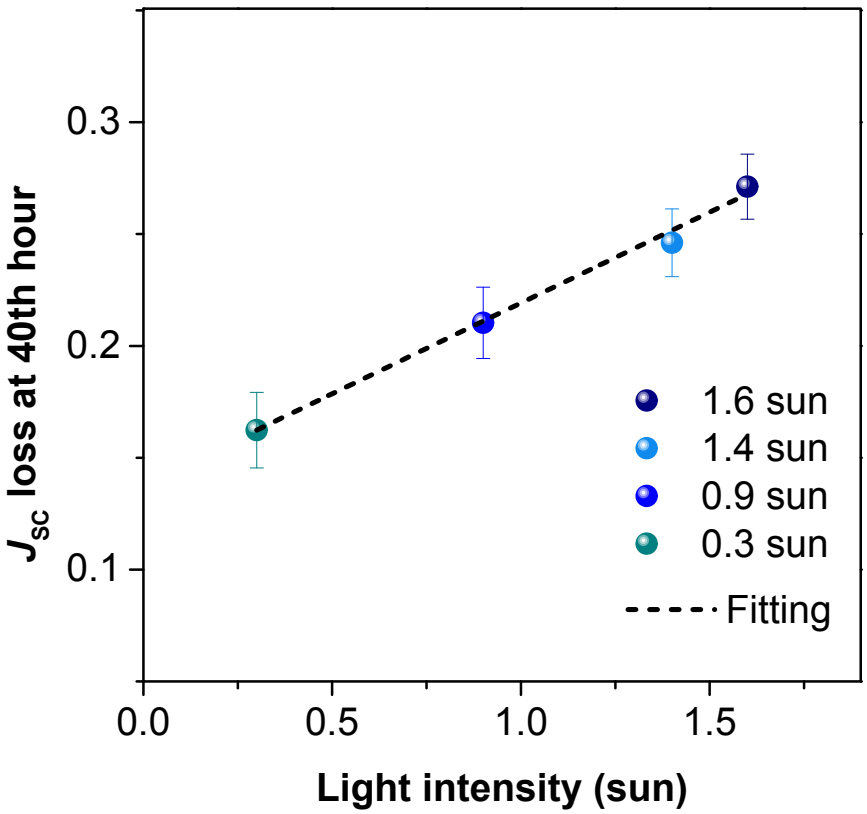

Figure S4. J_{SC} loss at 40th hour as a function of light intensity. Values were taken from figure 1e.

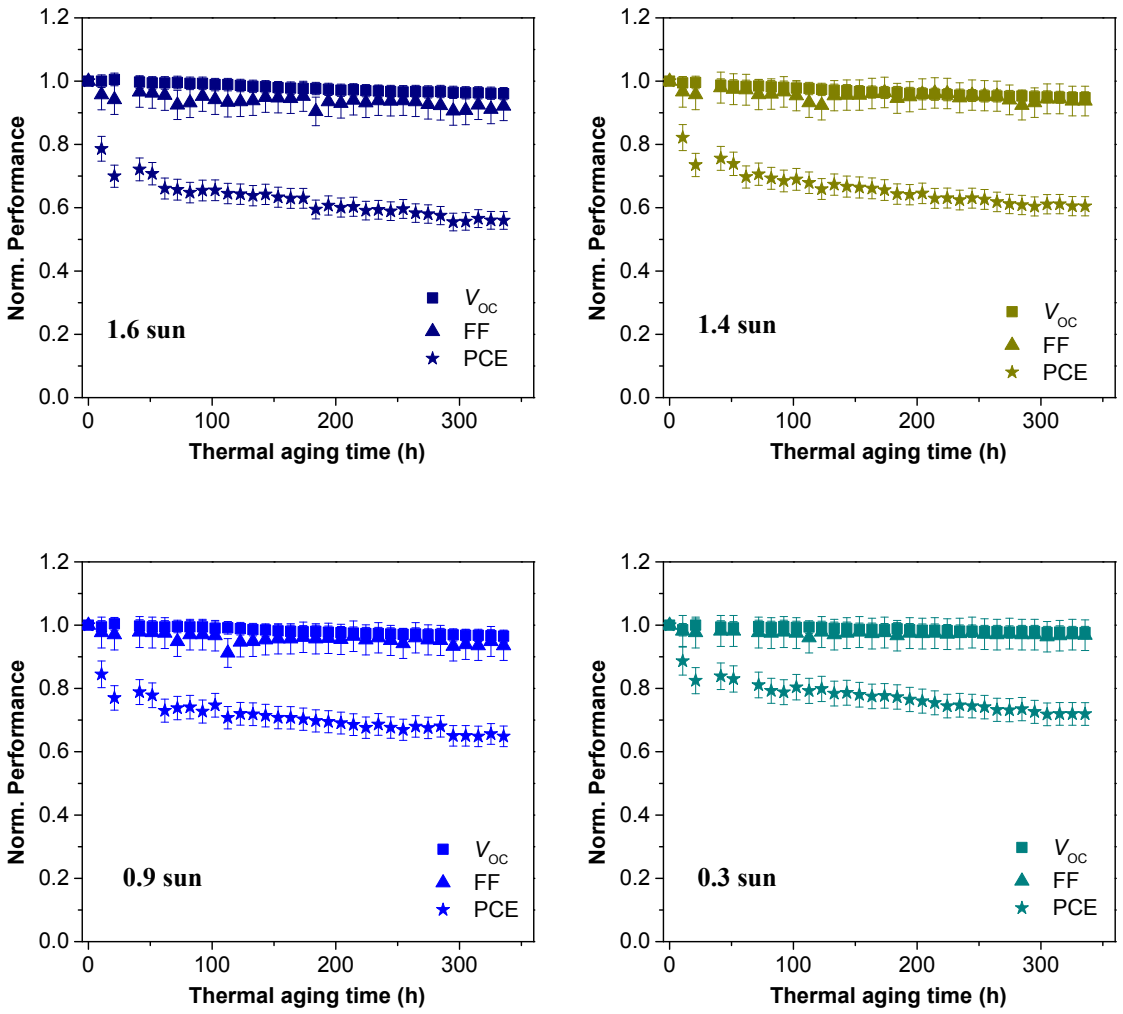

Figure S5. Normalized V_{OC}, FF and PCE evolution of PCE11:$PC_{71}BM$ solar cells aged under different light intensity in nitrogen atmosphere

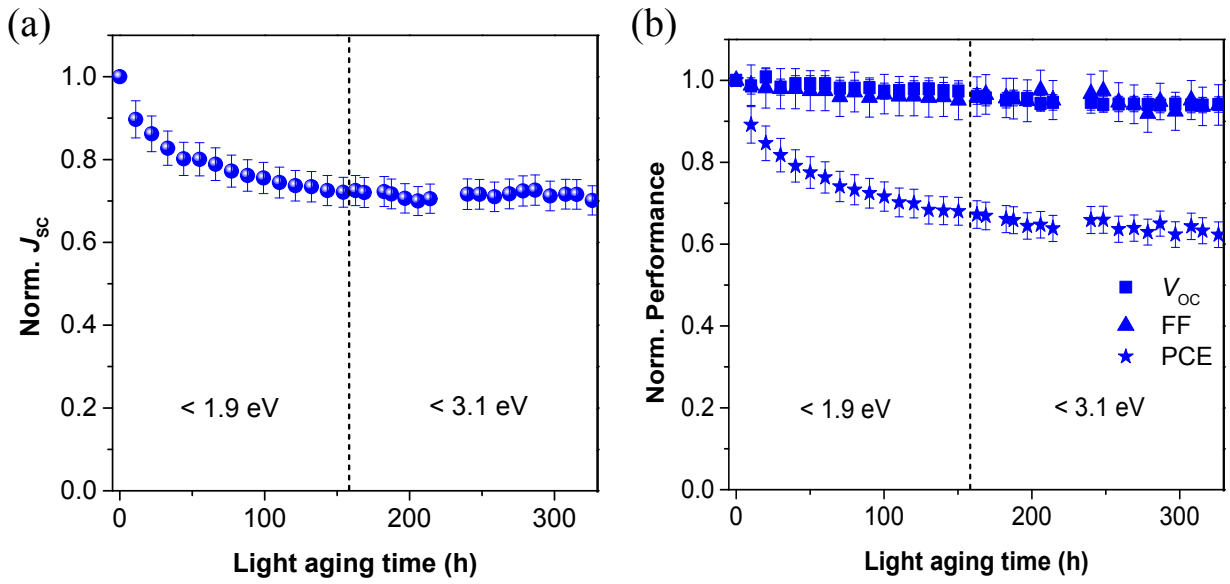

Figure S6. Normalized J_{SC}, V_{OC}, FF and PCE evolution of PCE11:$PC_{71}BM$ solar cells under light of different photon energy (~ one sun) in nitrogen atmosphere. The photon´s excess energy is the difference between the material bandgap and the photon energy. Light with an energy of 3 eV (about 413 nm) will dissipate more than 1.5 eV of heat when absorbed by a semiconductor with a bandgap of 1.5 eV (about 826 nm) That excess energy will dissipate heat into the lattice of the polymer by exciting phonon vibrations. Solar cells fabricated in the same run were tested under different light conditions.

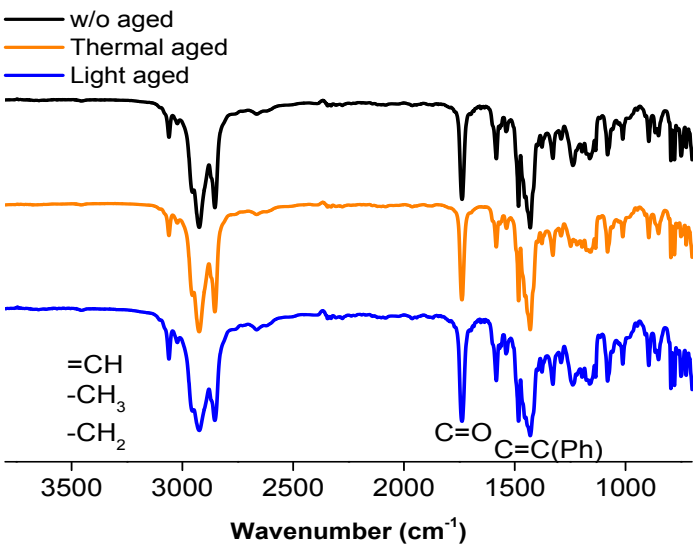

Figure S7. FTIR spectra of PCE11:PCBM composites with and without aging.

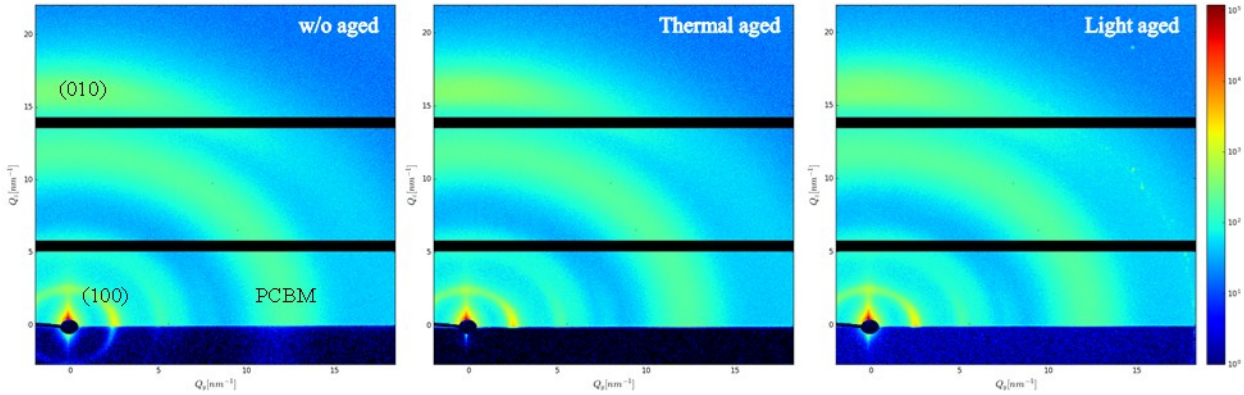

Figure S8. 2D GIWAXS patterns of PCE11:$PC_{71}BM$ blend films with and without aging. The color bars represent the intensity of the GIWAXS data. The import and export function of BoranAgain software[1] was used to depict the 2D patterns in Qy-Qz coordinate system.

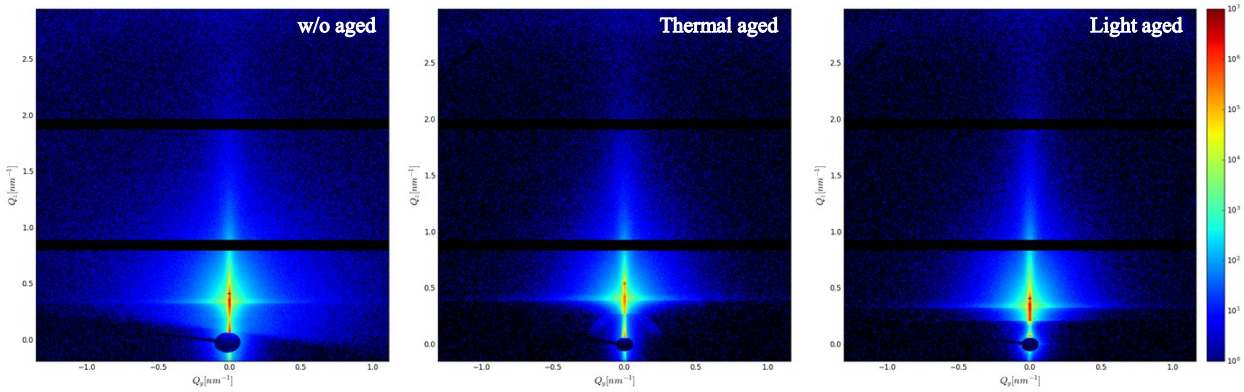

Figure S9. 2D GISAXS patterns of PCE11:PCBM blend films with and without aging. The color bars represent the intensity of the GISAXS data. The import and export function of BoranAgain software[1] was used to depict the 2D patterns in Qy-Qz coordinate system.

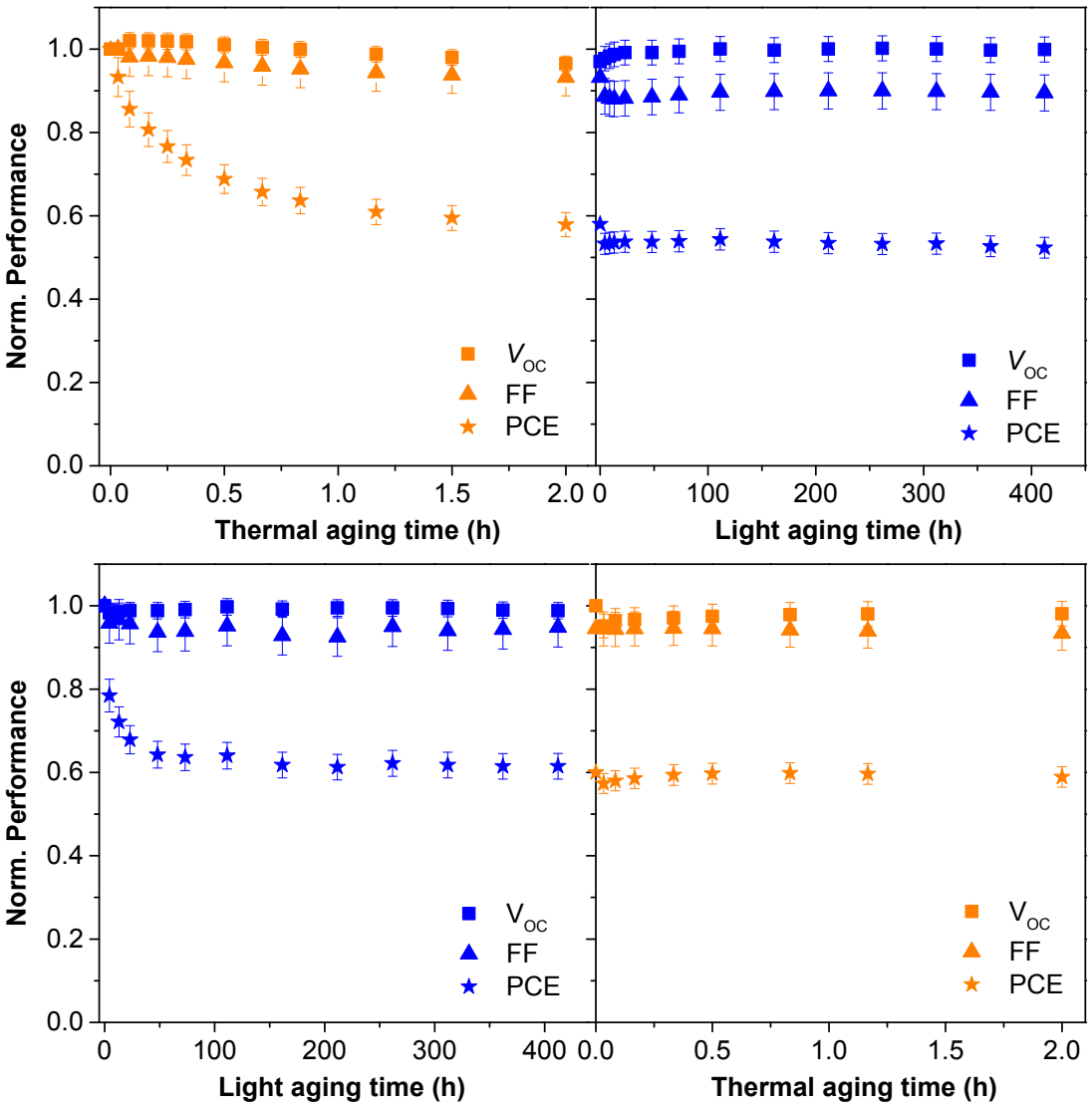

Figure S10. Normalized V_{OC}, FF and PCE evolution of PCE11:$PC_{71}BM$ solar cells during aging. Top: the solar cells were first under thermal aging at 85 °C then exposed to white light LEDs; Bottom: the solar cells were first under white light illumination then aged at 85 °C.

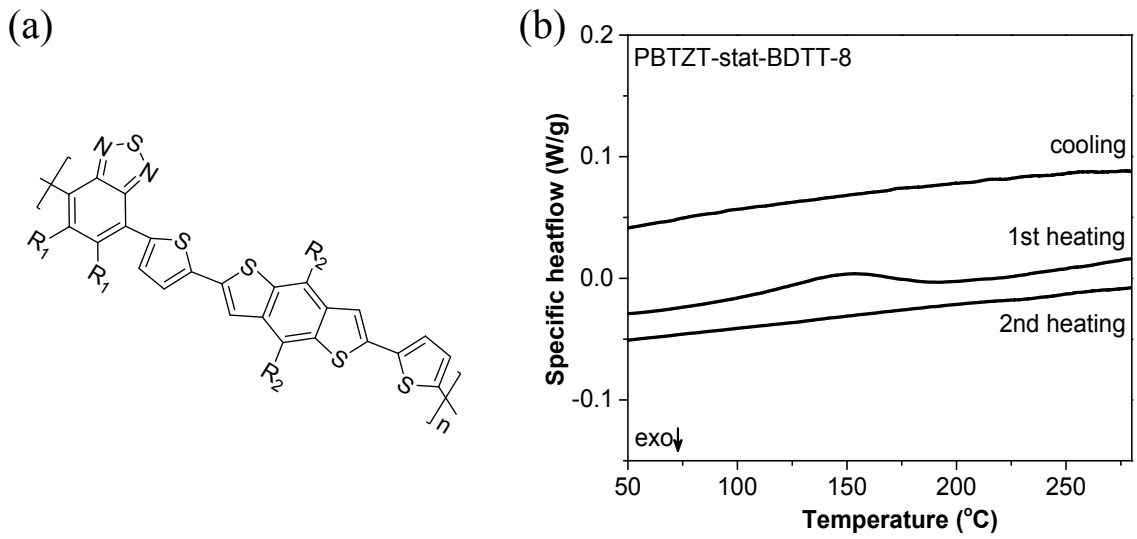

Figure S11. chemical structure (a) and DSC (b) of PBTZT-stat-BDTT-8 (P8). The sample was prepared by drop casting from chlorobenzene and dry under reduced vacuum overnight.

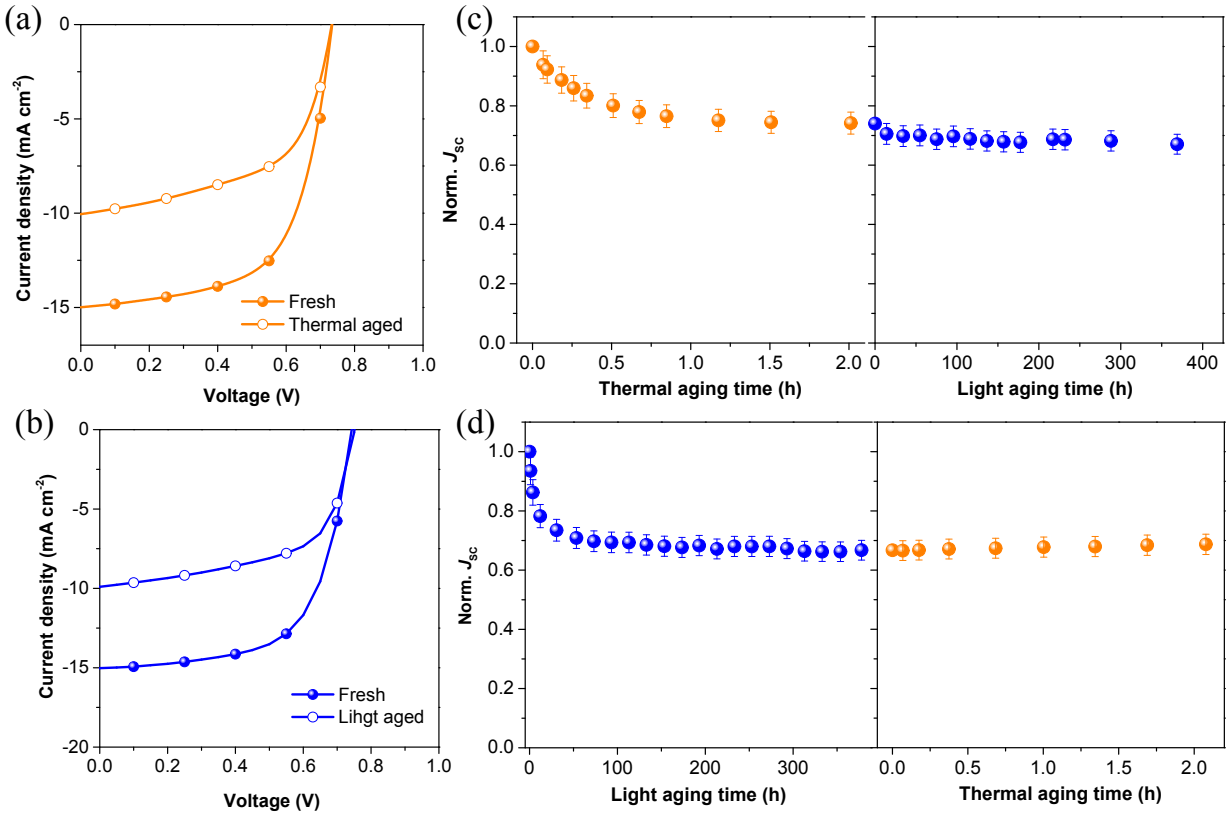

Figure S12. (a) and (b) Current density-voltage characteristics of fresh and aged PBTZT-stat-BDTT-8:$PC_{71}BM$ solar cells; (c) and (d) Normalized J_{SC} evolution of PBTZT-stat-BDTT-8:$PC_{71}BM$ solar cells during aging. (c): the solar cells were first under thermal aging at 85 °C then exposed to white light LEDs; (d): the solar cells were first under white light illumination then aged at 85 °C.

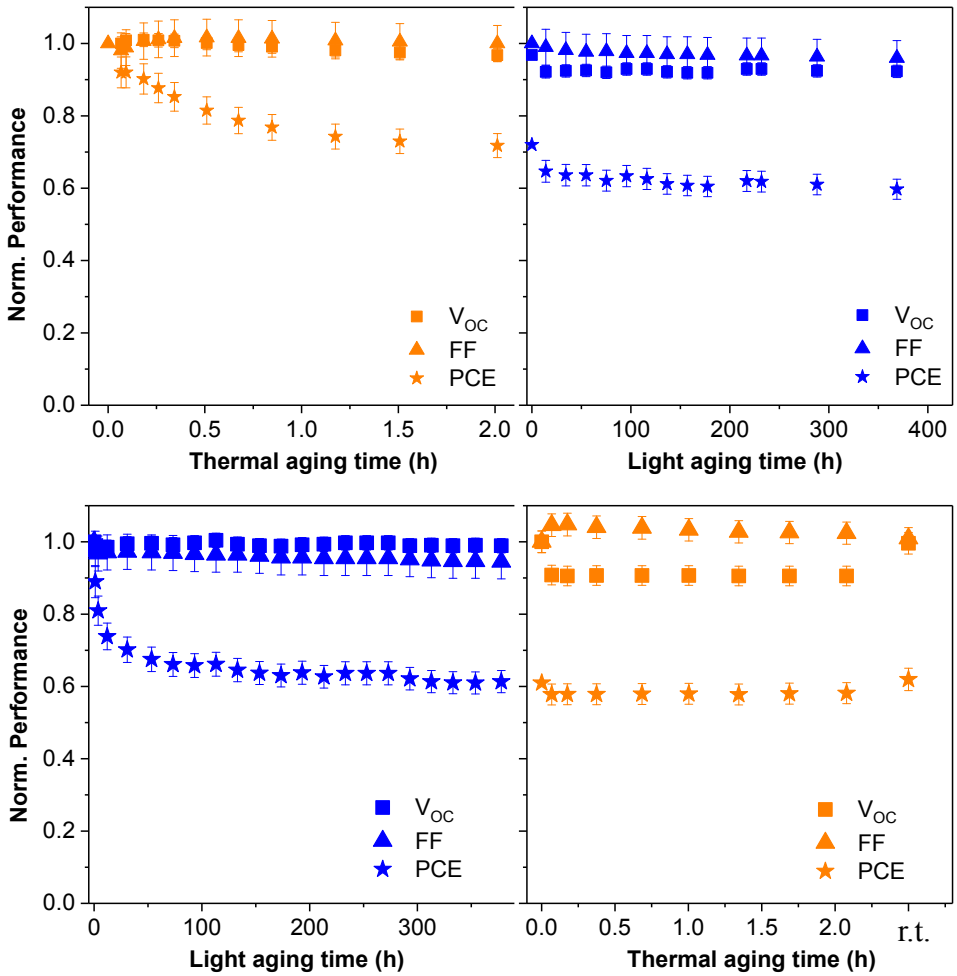

Figure S13. Normalized V_{OC}, FF and PCE evolution of PBTZT-stat-BDTT-8:$PC_{71}BM$ solar cells during aging. Top: the solar cells were first under thermal aging at 85 °C then exposed to white light LEDs; Bottom: the solar cells were first under white light illumination then aged at 85 °C.

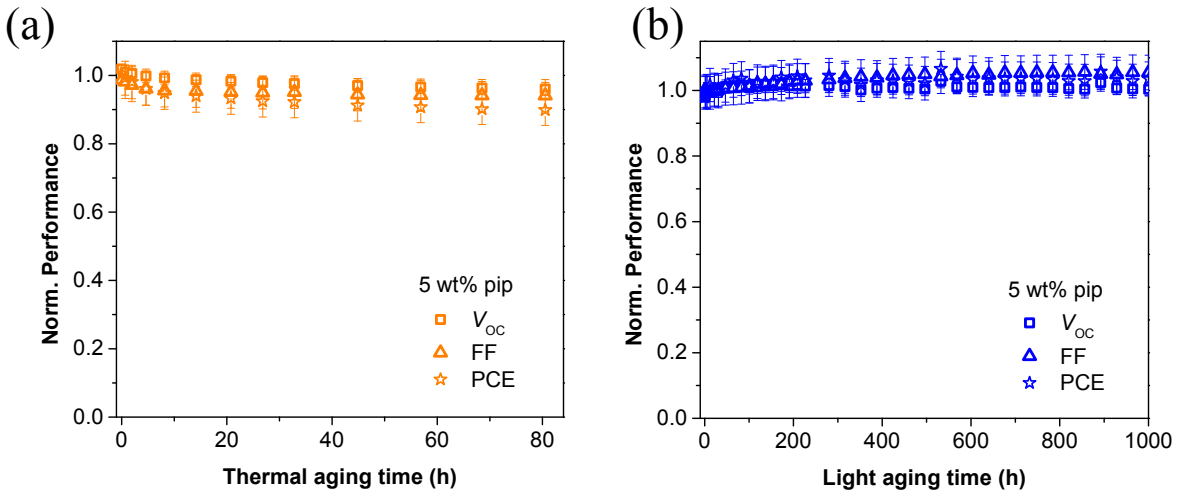

Figure S14. Normalized V_{OC}, FF and PCE evolution of PCE11:$PC_{71}BM$ solar cells with piperazine at 65 °C annealing (a) and under white light illumination (b) (~ one sun).

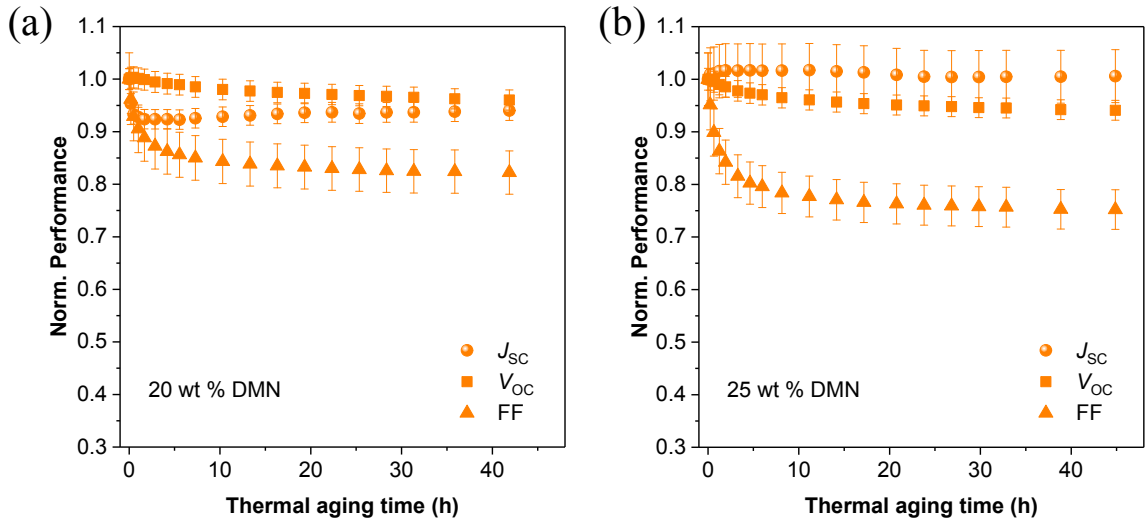

Figure S15. Normalized J_{SC}, V_{OC}, and FF evolution of PCE11:$PC_{71}BM$ solar cells under 65 ºC thermal aging; (a) with 20 wt% DMN, (b) with 25 wt% DMN.

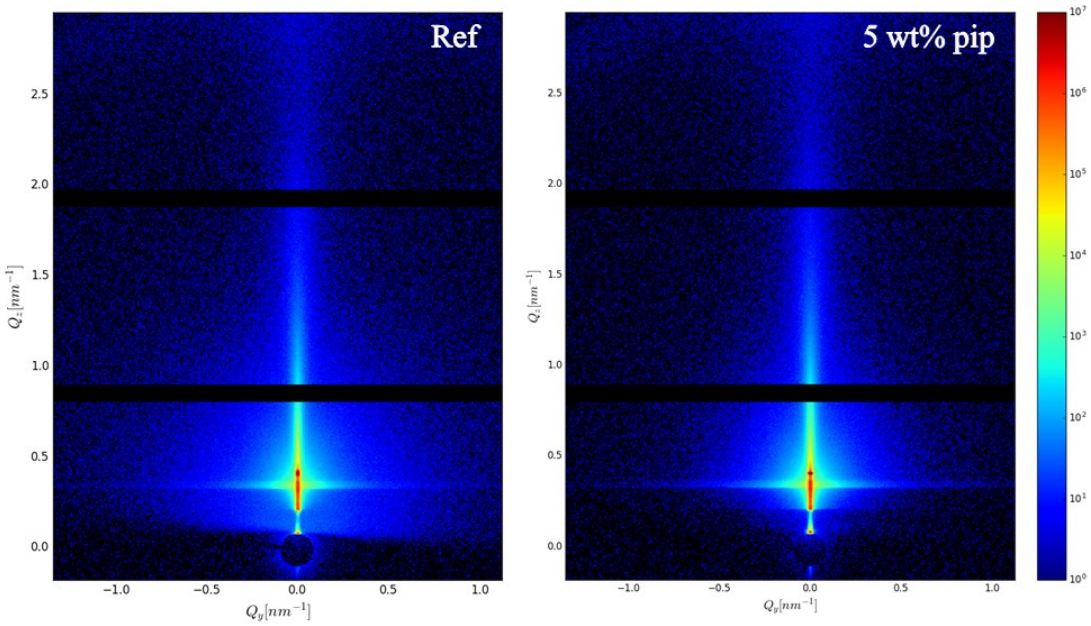

Figure S16. 2D GISAXS patterns of PCE11:PCBM blend films with and without piperazine. The color bars represent the intensity of the GISAXS data. The import and export function of BoranAgain software[1] was used to depict the 2D patterns in Qy-Qz coordinate system.

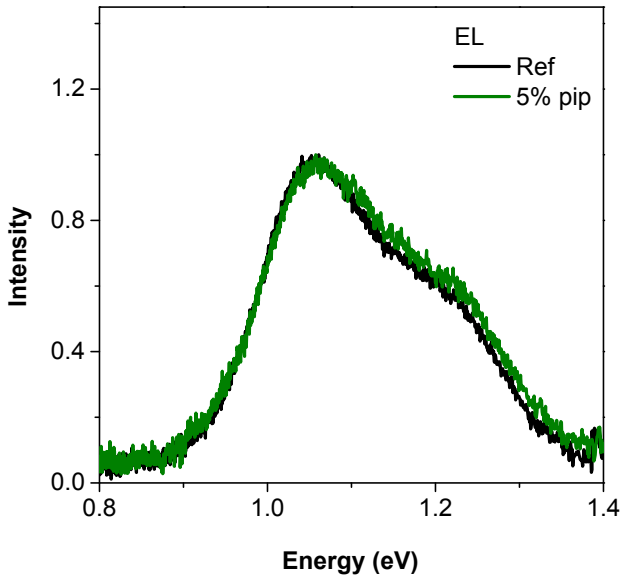

Figure S17. Charge transfer state of PCE11:PCBM solar cells without and with 5 wt% piperazine probed by means of electroluminescence spectroscopy.

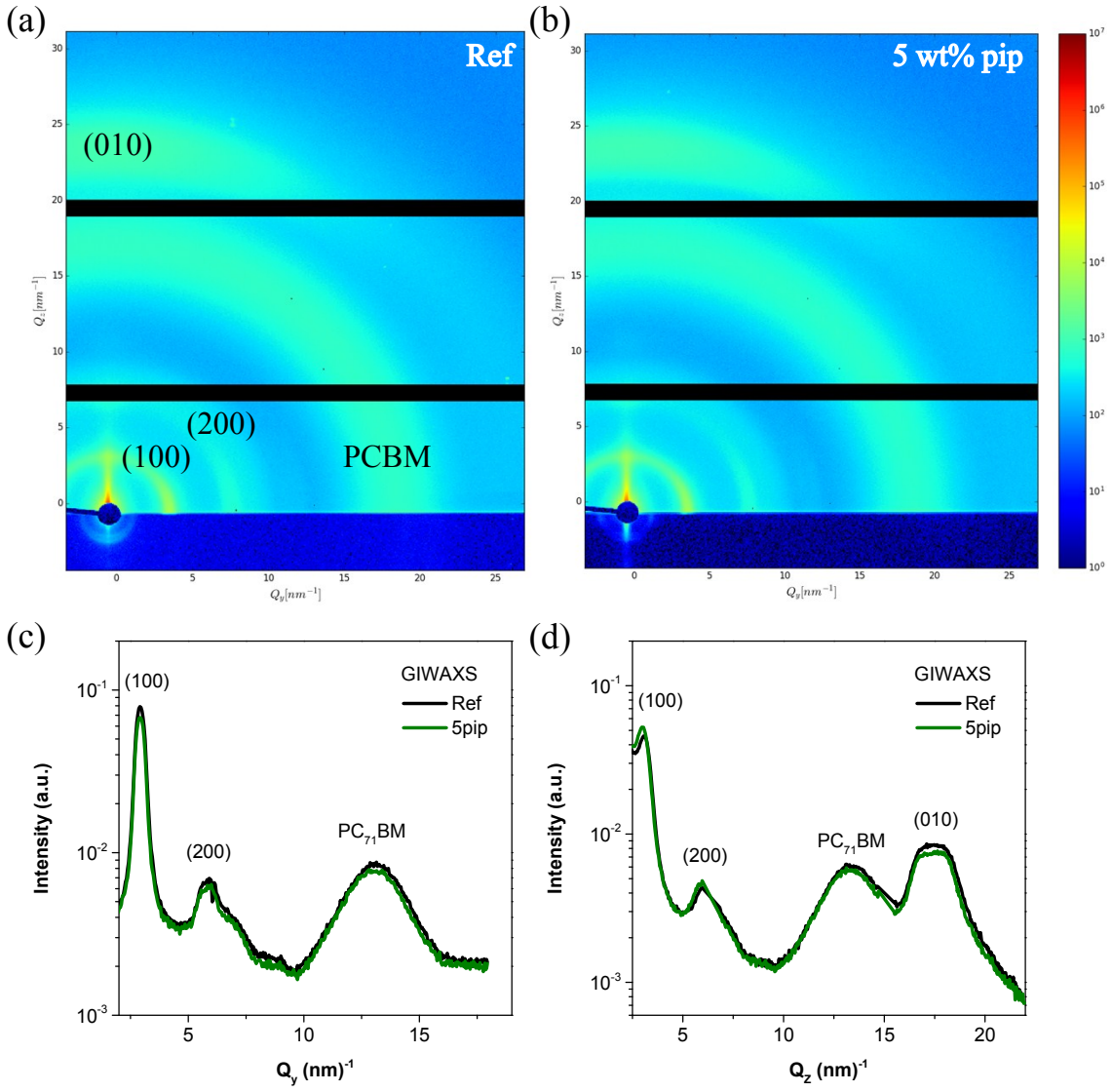

Figure S18. 2D GIWAXS patterns of PCE11:$PC_{71}BM$ blend films without (a) and with piperazine (b). The color bars represent the intensity of the GIWAXS data. The import and export function of BoranAgain software[1] was used to depict the 2D patterns in Qy-Qz coordinate system. (c) in-plane and (d) out-of-plane GIWAXS linecuts of PCE11:$PC_{71}BM$ films without/with piperazine.

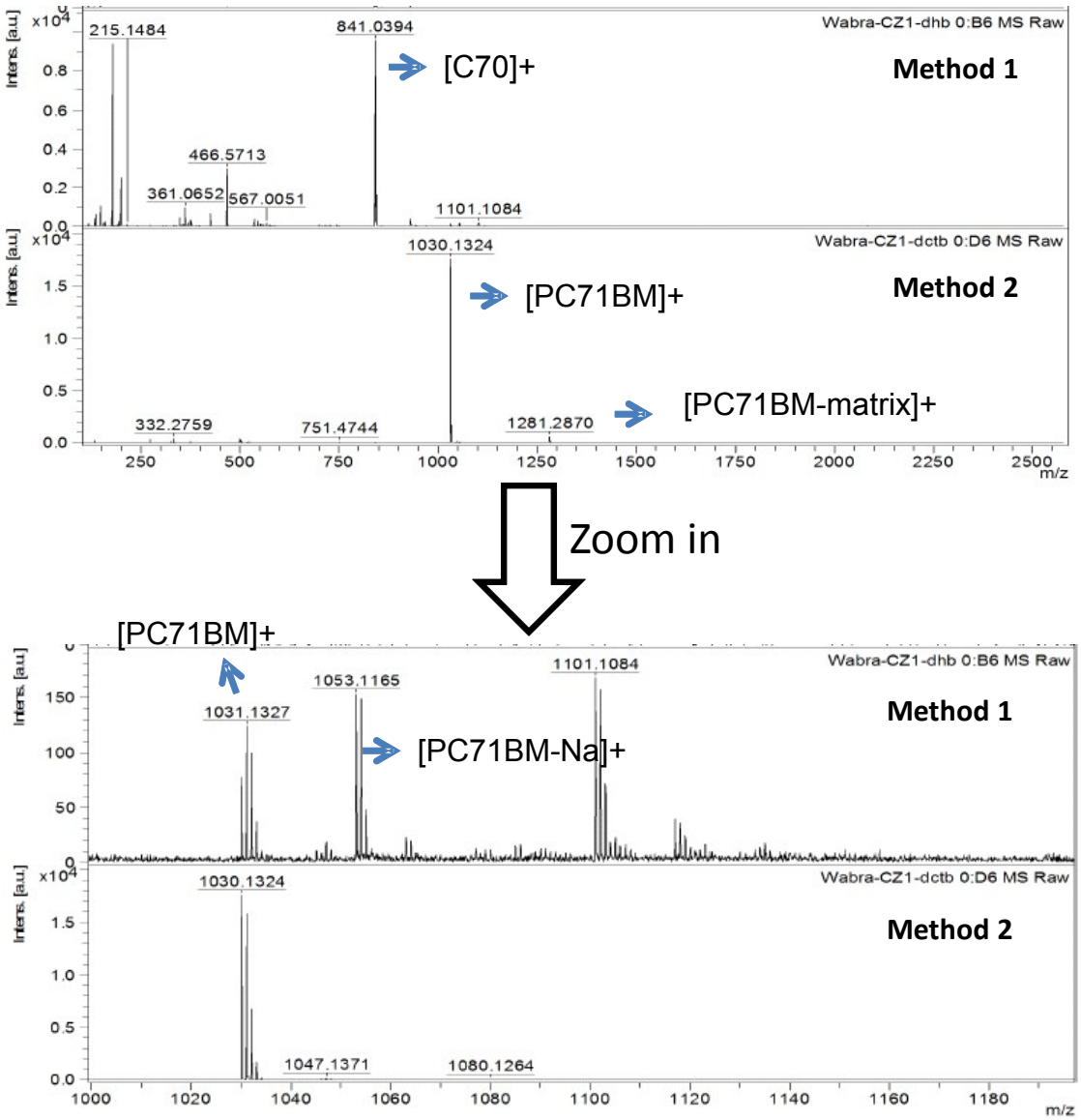

Figure S19. Mass spectrometry of $PC_{71}BM$ with 5 wt% piperazine. (Molecular weight of C_{70}, $PC_{71}BM$, and piperazine is 840, 1030 and 86, respectively). Sample preparation: $PC_{71}BM$:piperazine (100:5 in weight, 167:100 in mole) stir in chlorobenzene at 100 °C for 20 min (similar to method of making solution for solar cells); then the solution was dropcasted on glass substrates; 1.5 hour later, sample was dried under reduced pressure ($1*10^{-4}$ bar) for 1 hour. Attained solid was dissolved in toluene for characterization.

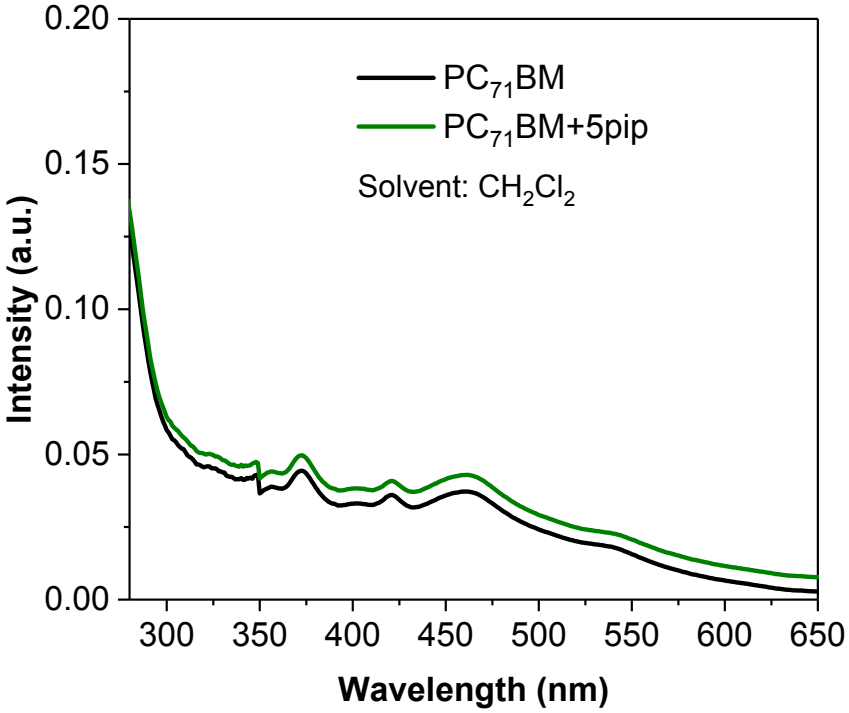

Figure S20. Absorption of pure $PC_{71}BM$ and $PC_{71}BM$ with 5 wt% piperazine. Sample with piperazine was under the same pre-process as in Figure S19.

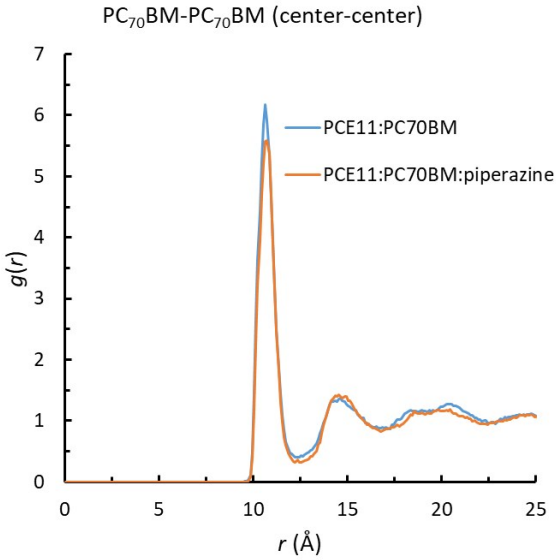

Figure S21. Radial distribution function between the $PC_{71}BM$ centers of mass.

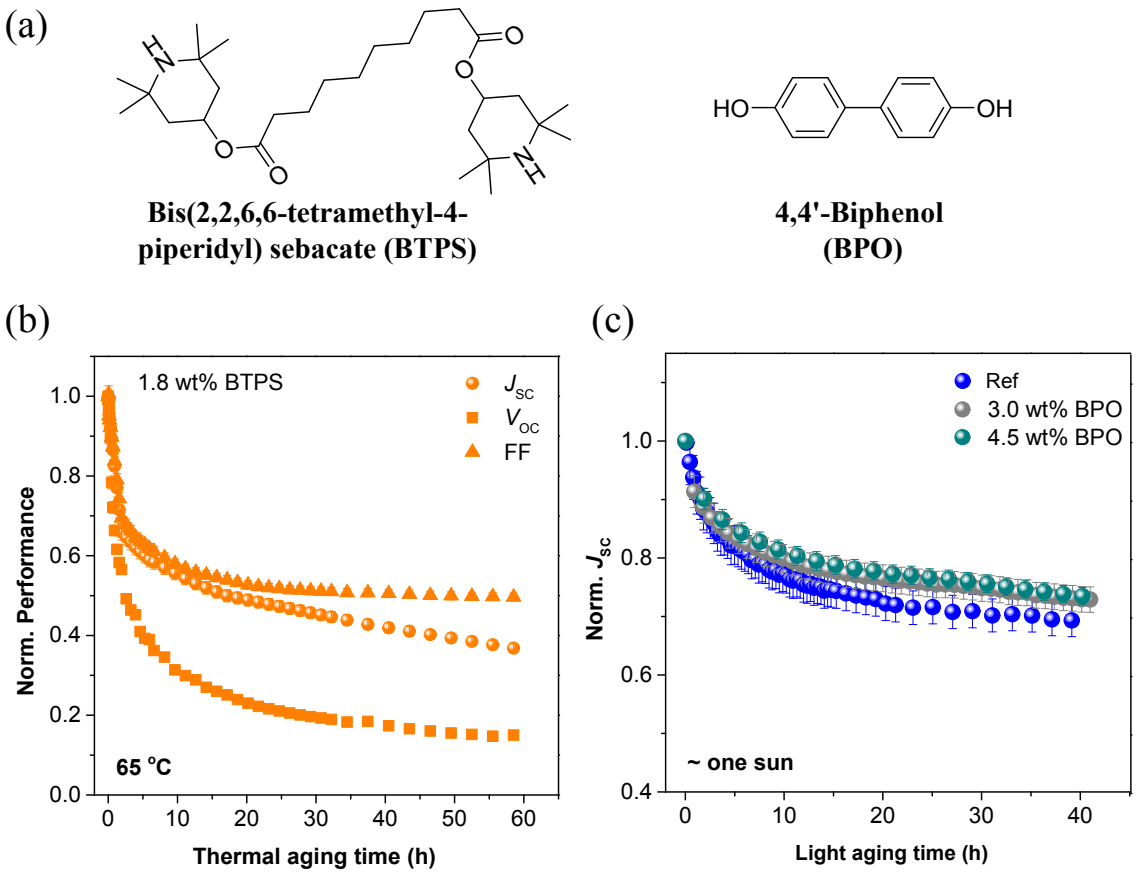

Figure S22. (a) Chemical structures of BTPS and BPO; (b) Normalized J_{SC}, V_{OC}, and FF evolution of PCE11:$PC_{71}BM$ solar cells under 65 °C thermal aging; (c) Normalized J_{SC} evolution of PCE11:$PC_{71}BM$ solar cells without/with BPO under one-sun white light illumination.

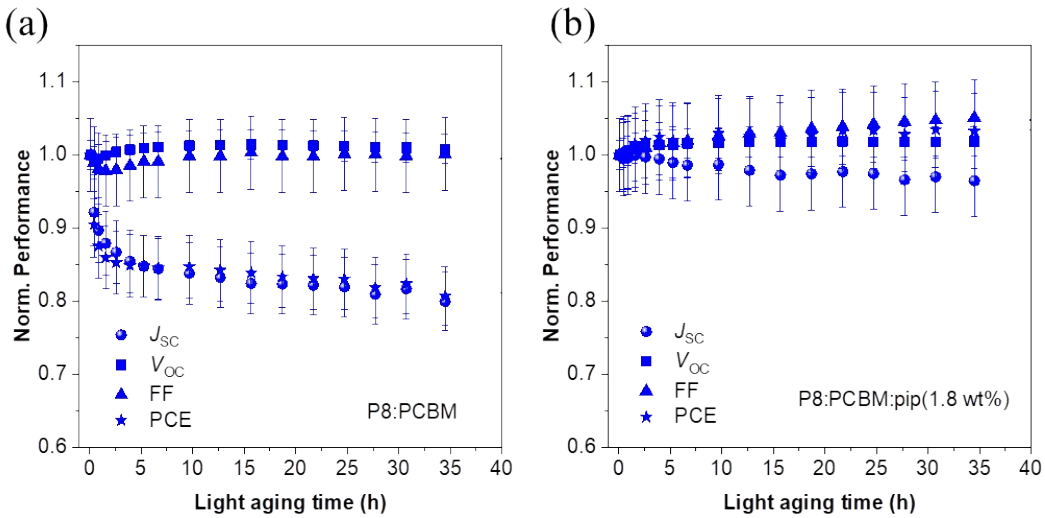

Figure S23. Normalized J_{SC}, V_{OC}, FF and PCE evolution of PBTZT-stat-BDTT-8 (P8) solar cells under illumination in nitrogen; (a) control solar cells, (b) solar cells with 1.8 wt% piperazine.

Table S1 Structural parameters determined by DAB model-fitting of GISAXS profiles of films with and without aging.

Sample	Correlation length[a)] of the mixed region (nm)	Standard deviation of the correlation length[b)] (nm)
w/o aged	9.4	1.16
thermally aged	10.02	0.37
light aged	11.64	0.3

[a)] Each sample was measured at three spots to account for lateral inhomogeneity. Given are the averaged values measured at three spots;

[b)] Given are the standard deviations of the three individual measurements.

The in-plane profiles of three samples were fitted with Debye-Anderson-Brumberger (DAB) model, and with a combined model of DAB model and poly-dispersed spheres having a Schultz-Zimm size distribution. The poly-dispersed spheres are supposed to describe the PCBM aggregates while the DAB model describes the large scale network of

the PCBM molecules distributed within the amorphous and around the crystalline polymer molecular conformations.[2] However, the contribution of the poly-dispersed spheres is so small that no reliable data can be extracted from the fits. Therefore, we restrict ourselves to the DAB model.

Table S2 Hansen Solubility Parameters, melting point, chemical structure and price of 21 additives

Material	δ_d **(MPa$^{1/2}$)**	δ_p **(MPa$^{1/2}$)**	δ_{hb} **(MPa$^{1/2}$)**	δ_T *a)* **(MPa$^{1/2}$)**	T_m **(°C)**	**Chemical structure**	**Price** *b)* **($/g)**
1,4-Piperazine	17.3	4.8	6	18.93	109	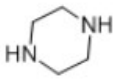	0.26
Dimedone	18.16	13.5	4.13	23.00	146	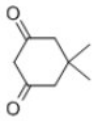	1.8
Hydrazobenzene	20.36	5.76	9.17	23.06	123	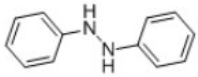	2
1,3,5-Tribromobenzene	20.52	8.43	5.77	22.92	117	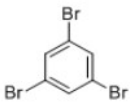	2
p-Diiodobenzene	21.07	3.96	6.2	22.32	131		3.5
1,2,4,5-Tetrachlorobenzene	21.2	10.7	3.4	23.99	139	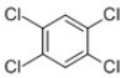	4
1,3-Dicyanobenzene	19.72	13.71	2.78	24.18	163	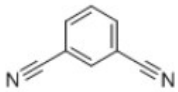	4
4,4'-Bipyridine	20.2	7.5	5.71	22.29	109	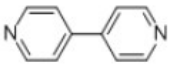	6

Terephthaldicarboxaldehyde	19.69	10.08	8.08	23.55	114	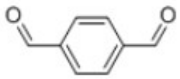	6
p-Dinitrobenzene	19.98	11.35	5.23	23.57	170	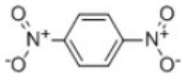	10
Carbon Tetraiodide	21.32	5.29	4.49	22.42	168		12
1,4-Dithiane	19.7	7.98	6.37	22.19	107		13
3,4,5,6-Tetrachlorobenzene-1,2-Dicarbonitrile	20.92	9.41	1.74	23.00	249	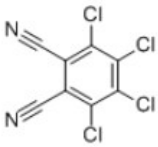	26
1,2-Dinitrobenzene	20.6	11.6	3.9	23.96	116	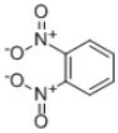	29
Hexamethyl Benzene	19.2	1.6	0	19.27	165	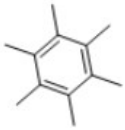	37
2,6-Dimethylnaphthalene	19.38	1.07	4.21	19.86	106	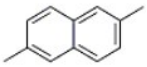	41
2,3-Dimethylnaphthalene	19.38	1.07	4.21	19.86	103	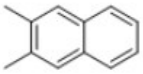	54
2,5-Dimethylpiperazine	17.07	5.82	6.52	19.18	113	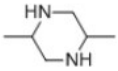	86
Decachlorobiphenyl	21.95	3.54	1.22	22.27	310	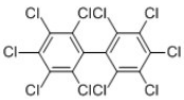	760

2,3,5,6-Tetramethyl phenol	18.5	2.13	7.62	20.12	117	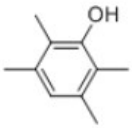	-[c)]
1,2,4,5-Tetrachloro-3,6-Dimethylbenzene	19.55	1.26	1.85	19.68	172	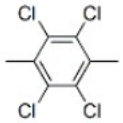	-[c)]

[a)] $\delta_T = \sqrt[2]{\delta_d^2 + \delta_p^2 + \delta_{hb}^2}$

[b)] Price is from Sigma-Aldrich; [b)] Price could not be found.

Table S3. Hansen solubility parameters (δ_d, δ_p, and δ_{hb}) and interaction parameter (χ_{12})

Materials/ Systems	δ_d **(MPa$^{1/2}$)**	δ_p **(MPa$^{1/2}$)**	δ_{hb} **(MPa$^{1/2}$)**	δ_T [b)] **(MPa$^{1/2}$)**	$\chi_{12} \cdot \frac{v_0}{RT}$ [c)] **(MPa)**
BTPS [a)]	16.63	2.63	2.17	16.98	–
BPO[a)]	20.68	6.58	13.46	25.54	–
PCE11-BTPS	–	–	–	–	4.67
PCE11-BPO	–	–	–	–	40.96

[a)] data from software HSPiP;[3]

[b)] $\delta_T = \sqrt[2]{\delta_d^2 + \delta_p^2 + \delta_{hb}^2}$

[c)] $\chi_{12} \approx \frac{v_0}{RT}(\delta_{T1} - \delta_{T2})^2$

where v_0 is the lattice site volume and is defined by the smallest unit; δ_1 and δ_2 are the Hildebrand solubility parameters of the fullerenes and the polymer, respectively; R is the ideal gas constant (8.314 cm^3 MPa K^{-1} mol^{-1}) and T the temperature (298 K).

Table S4. Hansen solubility parameters (δ_d, δ_p, and δ_{hb}) and interaction parameter (χ_{12})

Materials/ Systems	δ_d (MPa$^{1/2}$)	δ_p (MPa$^{1/2}$)	δ_{hb} (MPa$^{1/2}$)	δ_T [c)] (MPa$^{1/2}$)	$\chi_{12} \cdot \frac{v_0}{RT}$ [d)] (MPa)
PBTZT-stat-BDTT-8(P8) [a)]	18.50	3.90	3.10	19.16	–
Piperazine [b)]	17.30	4.80	6.00	18.93	–
P8-piperazine	–	–	–	–	0.23

[a)] data from reference[4]; [b)] data from software HSPiP[3]

[c)] $\delta_T = \sqrt[2]{\delta_d^2 + \delta_p^2 + \delta_{hb}^2}$

[d)] $\chi_{12} \approx \frac{v_0}{RT}(\delta_{T1} - \delta_{T2})^2$

where v_0 is the lattice site volume and is defined by the smallest unit; δ_1 and δ_2 are the Hildebrand solubility parameters of the fullerenes and the polymer, respectively; R is the ideal gas constant (8.314 cm^3 MPa K^{-1} mol^{-1}) and T the temperature (298 K).

References

1. C. Durniak, M. Ganeva, G. Pospelov, W. Van Herck and J. Wuttke, *version 1.9*, 2015, http://www.bornagainproject.org.

2. T. L. Lin, U. Jeng, C. S. Tsao, W. J. Liu, T. Canteenwala and L. Y. Chiang, *The Journal of Physical Chemistry B*, 2004, **108**, 14884-14888.

3. Abbott, S. J., Hansen, C. M. Hansen Solubility Parameters in Practice (software); www.hansen-solubility.com (accessed February 2017).

4. C. Zhang, S. Langner, A. V. Mumyatov, D. V. Anokhin, J. Min, J. D. Perea, K. L. Gerasimov, A. Osvet, D. A. Ivanov, P. Troshin, N. Li and C. J. Brabec, *Journal of Materials Chemistry A*, 2017, **5**, 17570-17579.